

Diamond in Surface Acoustic Wave Sensors

M.F. HRIBŠEK*, S.S. RISTIĆ AND B.M. RADOJKOVIĆ

Institute Goša, Milana Rakića 35, 11000 Belgrade, Serbia

The application of diamond in surface acoustic wave sensors is considered. The new method of the complete analyses of diamond-based gas chemical sensors is presented. It is based on the electromechanical equivalent circuit of the surface acoustic wave sensor. The method is very efficient and can be used for the optimal design of gas sensors. Since the diamond can be easily merged into solid state and biological systems, the development of smart biological sensors is possible. The advantages over silicon based sensors are also shown.

PACS numbers: 72.50.+b, 77.65.Dq, 43.35.Pt, 77.55.hd, 77.55.H-

1. Introduction

Since their invention in 1965 surface acoustic wave (SAW) devices have found numerous applications. [1–3]. Surface acoustic wave devices are based on Rayleigh wave motion along the surface of a piezoelectric material. One of the most important properties of the substrate material is the wave propagation velocity. The wave propagation velocity determinates operating frequency and dimensions of the device. Recently, multilayered substrates are used for the wave velocity increase [4]. The highest velocities are achieved when the piezoelectric material is placed on the top of the diamond layer, due to its highest acoustic wave velocity (10750 m/s) [5–13]. Several piezoelectric materials [5] in combination with diamond/silicon substrates have been investigated theoretically and experimentally. Theoretical calculation of the wave velocity in the multilayer structures is based on the solution of the wave equation [4, 14–15] demanding elaborate numerical computations. The use of diamond in the multilayered SAW structure has the following advantages: high frequencies up to 5 GHz, high coupling coefficients up to 1.2%, small temperature deviations, high power capability and small device size. The disadvantages of the layered SAW structures are the complex design and the problem related to the deposition of a piezoelectric layer with appropriate crystalline orientation. These facts probably result in little research on diamond-based SAW sensors [5]. Extreme chemical stability and bio-inertness [16] make diamond ideal material for sensors operating in harsh or biologic environments.

In the last two decades SAW chemical vapor sensors have found numerous applications due to their compact structure, high sensitivity, small size, outstanding stability, low cost, fast real-time response, passivity, and above all their ability to be incorporated in sophisticated mon-

itoring and measurement systems [1]. In order to make the whole system as compact as possible, the SAW device should be incorporated in complementary metal-oxide-semiconductor (CMOS) or micro-electro-mechanical system (MEMS) integrated circuits (IC) [4, 17]. In that case piezoelectric material is placed on the top of the IC circuit, e.g. on the top of silicon or the isolating layer, usually silicon dioxide.

One of the main objectives in a chemical sensor analysis is derivation of formulas which connect the change of electrical signals (e.g., voltages and frequency shifts) and chemical quantities (e.g., vapor concentration). The existing analysis approaches are based on the exact solution of the wave equation [4, 14–16, 18].

In this paper, a new modeling algorithm for the complete analysis of chemical SAW sensors with diamond layer placed on the top of silicon IC is presented. The algorithm, based on the electromechanical equivalent circuit method, consists of two parts. In the first part, the wave velocity of the SAW structure is derived in a closed-form expression. The wave velocity is calculated using an equivalent mechanical model of the multilayered delay line, analogy between the mechanical and electrical quantities and the fact that the surface wave practically propagates only in the upper, one wavelength thick layer of the substrate.

In the second part of the algorithm explicit general relations between electrical signals, voltages or frequencies, and vapor detection estimations are presented.

2. Chemical SAW Sensors with a diamond layer

Typical position of a diamond layer in a transversal SAW sensor, or delay line SAW sensor, in a silicon integrated circuit is schematically presented in Fig. 1. The substrate consists of three layers. The bottom layer is silicon (or silicon with a thin layer of silicon dioxide), the middle layer is diamond and the top layer is a piezoelectric material. The thickness of the diamond layer

* corresponding author; e-mail: marija.hribsek@yahoo.com

must be large enough so that the silicon substrate has no (or a negligible) influence on the acoustic propagation and the diamond can be assumed as semi-infinite. In order to benefit from the favorable properties of diamond, the thickness of the piezoelectric layer should be much smaller than the diamond layer. In chemical SAW sensors between the input and output interdigital transducers (IDT) on the top of the piezoelectric material a chemically sensitive thin layer is placed. Piezoelectric materials are anisotropic. Commonly used piezoelectric materials in classical SAW applications are ST-cut quartz and lithium niobate. Recently, ZnO, AlGa_N, GaN, AlN are used in MEMS technology and in systems compatible with CMOS technology [4, 17, 19–21].

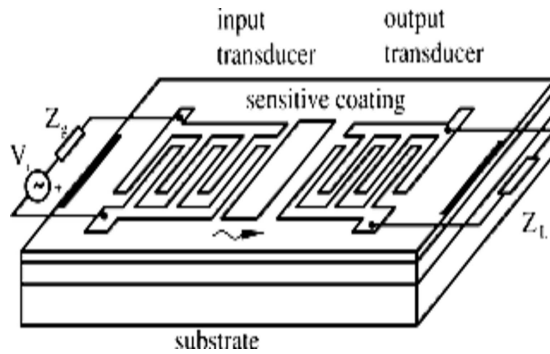


Fig. 1. Basic structure of a chemical SAW sensor with a diamond layer.

The surface wave is induced by an electrical signal applied to the input IDT. The output signal is taken from the output IDT. The velocity of the wave is sensitive to mass and viscosity of the sensing thin layer. The sensing layer is usually a polymer film and it absorbs volatile chemical compounds of interest. When the gas is absorbed, the mass of the polymer increases causing a change in velocity and phase of the acoustic signal, which implicates a frequency change of the output voltage at the impedance $Z_L = R_L$. The IDT is bi-directional: it launches the wave on both sides equally. Acoustic absorbers are placed on the substrate edges, dark lines in Fig. 1, to eliminate the reflection from the edges of the substrate. The IDTs are identical with uniformly spaced metal electrodes, usually aluminum (Al), of equal lengths and equal ratio of electrodes l width and spacing. The number of electrodes defines the frequency bandwidth of a SAW device. The electrode's length and number, and coupling networks at the electrical ports, if needed, should be chosen to match the IDT input resistance, at the center frequency f_0 , to the load resistance R_L and the generator resistance R_g . The wavelength corresponding to the center frequency equals the distance between the electrodes of the same polarity. The center frequency is determined by the IDT's geometry and the wave velocity in the piezoelectric material.

3. New method of complete analyses of gas chemical diamond-based sensors

The first step in the analyses is the calculation of the center frequency f_0 . It is calculated from the well-known formula [3]:

$$f_0 = v/\lambda \tag{1}$$

where v is the phase wave velocity and λ the wavelength. The wavelength λ is determined by the periodicity of the electrodes, but v must be calculated. The exact method of the calculation is the solution of the wave equation which involves the tedious numerical computations even in the single layer substrate [4, 22].

The new method of a two-layer substrate velocity calculation presented in this paper is much simpler. It is based on the mechanical equivalent scheme of the layers between the transducers, which is actually a delay line. The input velocity of the delay line is the same for the substrate plane normal to the direction of the wave propagation. Therefore, the mechanical impedances of the layers are connected in series. Figure 2 represents the mechanical equivalent scheme of the delay line input, where F is the force. Z_u and Z_d represent the characteristic impedances of the piezoelectric and diamond layer, respectively, defined by:

$$Z_u = h_u w \rho_u v, \tag{2}$$

$$Z_d = \lambda w \rho_d v, \tag{3}$$

where ρ_u and ρ_d are the mass densities of the layers, h_u is the height of the upper layer and w is the width of the layers.

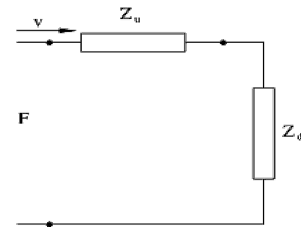


Fig. 2. Equivalent mechanical circuit of the delay line input for a two-layer substrate.

In Eq. (3), instead of the real layer thickness, λ is used, because the surface wave practically propagates only in the upper, one wavelength thick layer of the substrate [3, 22]. From Eq. (2) the wave velocity is calculated using analogy between the mechanical and electrical quantities [23].

$$v = \frac{v_d}{1 + \frac{Z_u}{Z_d}} = \frac{v_d}{1 + \frac{h_u \rho_u}{\lambda \rho_d}}, \tag{4}$$

where v_d is the wave velocity of the diamond without the upper layer. The velocity is derived in a closed-form expression which is very convenient.

The next step in the analyses is to find the straightforward connection between the change of the output electrical signals (e.g., voltage and frequency) and detected

chemical quantities (e.g., vapor concentration). Using the expressions developed in [23] the concentration of the detected gas can be found as:

$$C_v = \frac{\Delta f_{\text{vap}} \rho_s v}{K h_p f_0^2} = \frac{\Delta f_{\text{vap}} \rho_s \lambda^2}{K h_p v}, \quad (5)$$

where Δf_{vap} is the deviation from the center frequency in the presence of the gas, ρ_s is the density of the piezoelectric substrate, h_p is the thickness of the sensing material (polymer film), and K is the partition coefficient between the concentration of the chemical compound in sorbent phase (in the sensing sorbent coating material) and vapor phase (concentration in the ambient) [23]. Vapor sensitivity depends on the choice of the sorbent material, polymer, and its strength of sorption, which is given by the partition coefficient K . The concentration in Eq. (5) is in g/cm^3 , density is in g/cm^3 , and all other quantities are in SI units. The value of K depends on the concentration units used.

Surface mass sensitivity S_m defined as the ratio of frequency deviation and the change in the surface mass is an important characteristic of a SAW sensor. Using (5) it can be found:

$$S_m = \frac{\Delta f}{\Delta(\rho_p h_p)} = \frac{1}{\rho_s v} f_0^2 = \frac{v}{\rho_s \lambda^2} \quad (6)$$

where $\rho_p = K C_v$.

From Eq. (6) it is very clear that for the same λ and substrate the mass sensitivity increases with velocity increase.

4. Results and discussion

Equation (4) is applied to the calculation of wave velocities for the cases: aluminum nitride (AlN) on silicon and AlN/diamond on silicon as reported in [21]. In the calculations, the following values are used: the wave velocity of diamond $v_d = 10750.80 \text{ m/s}$, the density of diamond $\rho_d = 3.52 \text{ g/cm}^3$, the density of AlN $\rho_{\text{AlN}} = 3.26 \text{ g/cm}^3$. According to Eq. (4), the velocity v as a function of the relative AlN film thicknesses h_{AlN}/λ is calculated and shown in Fig. 3 (\blacktriangle points). The simulation results are in a good agreement with the theoretical results reported in [21], where the velocities were found from the equation of motion using the PC Acoustic Wave Software from McGill University [24].

In the same figure the results for AlN/Si structure are presented (\blacksquare points). In the calculations, the following values are used: the wave velocity in silicon $v_{\text{Si}} = 4900 \text{ m/s}$, and the density of silicon $\rho_{\text{Si}} = 2.329 \text{ g/cm}^3$.

Figure 3 shows that the wave velocity of an AlN/diamond structure is greater than the velocity in a single AlN layer ($v_{\text{AlN}} = 5600 \text{ m/s}$, [6]), or AlN/Si structure. The increase of the wave velocity enables higher operating frequencies without submicron electrode manufacturing and higher sensor sensitivities.

For $\lambda = 8 \text{ }\mu\text{m}$ and $h_{\text{AlN}}/\lambda = 0.27$, the wave velocity is 8600 m/s and the center frequency is approximately 1075 MHz , which agrees almost perfectly with the theoretical data in [21]. The corresponding measured center

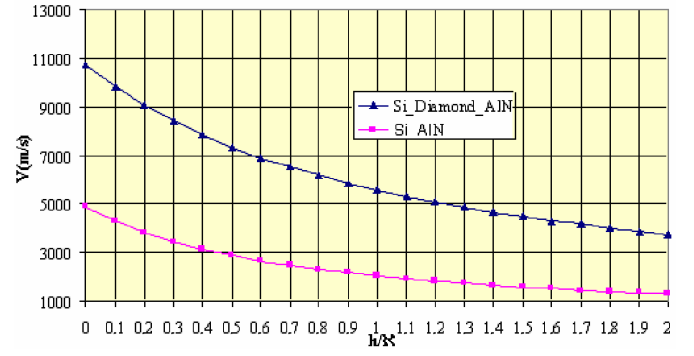


Fig. 3. Wave velocities of the Si/diamond/AlN, (\blacktriangle points), and Si/AlN, (\blacksquare points), structures.

frequency is about 1.3 GHz [21]. The disagreement of the measured and calculated data is probably the result of fabrication errors and the fact that in the model stiffness of the AlN film is assumed to be negligible. In sensor applications it is not needed to have the exact value of the center frequency (as it is in communication systems) since only its deviations are accounted for. The electrode width in this case is $2 \text{ }\mu\text{m}$, while in the case of quartz substrate for the same frequency it should be $0.73 \text{ }\mu\text{m}$. The electrode width versus frequency for the wave velocity of 8600 m/s in AlN/diamond structure is presented in Fig. 4 (\blacklozenge points). In the same figure, the corresponding function for ST quartz is presented (\blacksquare points).

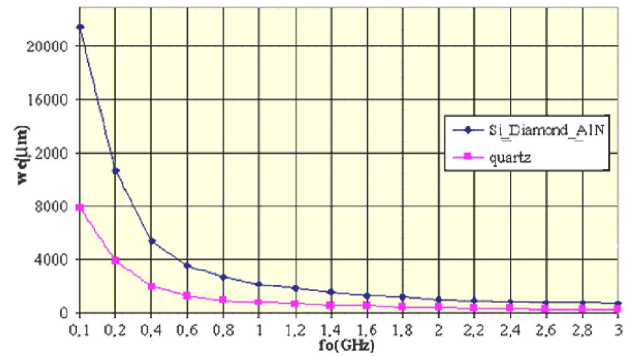


Fig. 4. Electrode width versus center frequency, \blacklozenge Si/diamond/AlN, \blacksquare quartz.

According to (6), AlN/diamond based sensors have approximately 2.3 times better mass sensitivity than quartz-based sensors for the same wavelength (5). Relative frequency changes versus gas concentrations of ethanol and CO sensor are calculated using (5) and presented in Fig. 5. The wave length is $8 \text{ }\mu\text{m}$ and the thicknesses of the AlN and diamond layers are 2.16 and $22 \text{ }\mu\text{m}$, respectively. The sensing layer of Co-tetra-phenyl-porphyrin is 10 nm thick [21].

It can be seen that the agreement with corresponding experimental data for the same sensor given in [21] is excellent for smaller concentrations.

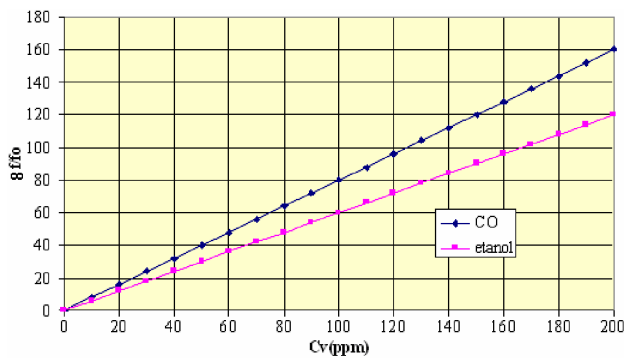


Fig. 5. Response curves for CO (◆ points), and Ethanol (■ points).

The same formula for concentration prediction is applied for the same AlN/diamond and transducers structure with sensing layer of polyepichlorohydrin (PECH) for detection of dichloromethane (CH_2Cl_2 , DCM), gas which is similar to warfare chemical agents. For 5 ppm concentration of DCM, the calculated frequency shift is 850 Hz. There are no experimental results for this case.

The only experimental results available for DCM detection are reported in [25] for quartz-based sensors. The experiments were carried out without any predictions, for quartz-based devices at the center frequencies of 39.6, 99, 132, 198, and 264 MHz, different polymers, and three gases which simulate warfare chemical agents. Polymers were polyisobutylene (PIB), polyepichlorohydrin (PECH), and polydimethylsiloxane (PDMS) deposited by the spin coating technique. Space between the transducers was $1500 \mu\text{m}$ with the aperture $1800 \mu\text{m}$. The characteristics were measured directly using E-5061 A network analyzer. For 5 ppm of DCM they measured frequency shift of 574 Hz for the device with center frequency of 264 MHz and thicker polymer films [25].

5. Conclusions

A new complete analyses method of SAW transversal gas chemical sensors on AlN/diamond substrate based sensors has been developed. The method is based on electromechanical equivalent circuits of a SAW delay line. The closed-form analytic expression for the wave velocity calculation of AlN/diamond structure is developed. The expression explicitly relates the wave velocity, the layer parameters, and the wavelength corresponding to the center frequency, which is the basic parameter of interdigital transducers design. The velocity is calculated much faster than in the usually used method which demands elaborate numerical computations.

The presented closed form analytic expression explicitly relates the vapor concentration, substrate parameters and center frequency. It enables insight into the influence of the sensor design parameters on the sensor

performance and predicts very efficiently and correctly frequency shifts due to the vapor concentrations.

The simulation results, based on the proposed expressions, are in a good agreement with the experimental results. The results presented facilitate SAW sensors analyses and can be used in the future for the more efficient design of optimal sensors, with respect to the sensor sensitivity or required area on the sensor chip.

Acknowledgments

This work was supported by the Ministry of Science and Technological Development of Serbia under Grant TR 11026.

References

- [1] A. Pohl, *IEEE Transactions on Ultrasonics, Ferroelectrics, and Frequency Control* **47**, 317 (2000).
- [2] E. Comini, G. Faglia, G. Sberveglieri, *Solid State Gas Sensing*, Springer Science+Business Media LLC, New York 2009.
- [3] M. Golio, *The RF and Microwave Handbook*, 2nd ed., CRC Press LLC, Boca Raton 2008.
- [4] S. Ahmadi, F. Hassani, C. Korman, M. Rahaman, M. Zaghoul, in: *Proceedings of the IEEE Conference on Sensors*, Vienna 2004, p. 1129.
- [5] V. Mortet, O.A. Williams, K. Haenen, *Phys. Stat. Sol.* **205**, 1009 (2008).
- [6] El Hakiki, M. Elmazria, O. Assouar, M.B. Mortet, Vincent Le Brizoual, L. Vanecek, M. Alnot, *Diamond & Related Materials* **14**, 1175 (2005).
- [7] S. Shikata, S. Fujii, T. Uemura, K. Itakura, A. Hachigo, H. Kitabayashi, H. Nakahata, Y. Takada, *New Diamond and Frontier Carbon Tehnology* **15**, 349 (2005).
- [8] M. Benetti, D. Cannatta'a, F.D. Pietrantonio, E. Verona, *IEEE Transactions on Ultrasonics, Ferroelectrics, and Frequency Control* **52**, 1806 (2005).
- [9] P. Kirsch, M.B. Assouar, O. Elmazria, M.E. Hakiki, V. Moret, P. Alnot, *IEEE Transactions on Ultrasonics, Ferroelectrics, and Frequency Control* **54**, 1486 (2007).
- [10] P. Kirsch, M.B. Assouar, O. Elmazria, V. Mortet, P. Alnot, *Appl. Phys. Letts.* **88**, 223504 (2006).
- [11] T. Omori, A. Kobayashi, Y. Takagi, K. Hashimoto, M. Yamaguchi, in: *Proceedings of Ultrasonics Symposium, 2008. IUS 2008. IEEE*, Beijing 2008, p. 196.
- [12] S. Besmaine, L.Le. Brizoual, M. Elmazria, J.J. Fundenberger, M. Belmahi, B. Benyoucef, *Diamond and Related Materials* **17**, 1420 (2008).
- [13] S. Jian, B. YiZhen, S. JingChang, D. GuoTong, J. Xin1, *Chinese Science Bulletin* **53**, 2931 (2008).
- [14] S. Sankaranarayanan, V.R. Bhethanabotla, B. Joseph, in: *Proc. of 208th ECS Meeting*, Eds: G. Hunter, P. Hesketh, C. Kranz, Los Angeles 2005, p. 19.
- [15] C.-C. Sung, Y.-F. Chiang, R. Ro, R. Lee, S. Wu, in: *Proceedings of Frequency Control Symposium*, IEEE International, Besancon 2009, p. 446.

- [16] C.G. Specht, O.A. Williams, R.B. Jackman, R. Schoepfer, *Biomaterials* **25**, 4073 (2004).
- [17] A. Zaki, H. Elsimary, M. Zaghoul, in: *Proceedings of the 5th WSEAS International Conference on Circuits, Systems, Electronics Control and Signal Processing*, Dallas 2006, p. 10.
- [18] S.J. Martin, G.C. Frye, S.D. Senturia, *Analytical Chemistry* **66**, 2201 (1994).
- [19] L. Rufer, T. Lalinský, D. Grobelný, S. Mir, G. Vanko, Zs. Őszi, Ź. Mozolová, J. Gregus, in: *Proceedings of the 6th International Conference on Advanced Semiconductor Devices and Microsystems, ASDAM 2006*, Smolenice 2006, p. 165.
- [20] M.B. Assouar, O. Elmazria, R. Jimenez, F. Sarry, P. Alnot, *Applied Surface Science* **164**, 200 (2000).
- [21] M. Benetti, D. Cannata, A. D'Amico, F. Di Pietrantonio, A. Macagnano, E. Verona, in: *Proceedings of the IEEE Conference on Sensors*, Vienna 753 (2004).
- [22] C. Campbell, *Surface Acoustic Wave Devices and their Signal Processing Applications*, Academic Press, San Diego 1989.
- [23] Z. Źivković, M. Hribšek, D. Tošić, *Informacije MI-DEM* **39**, 111 (2009).
- [24] E.L. Adler, J.K. Slaboszewicz, G.W. Farnell, C.K. Jen, *IEEE Transactions on Ultrasonics, Ferroelectrics, and Frequency Control* **37**, 215 (1990).
- [25] B.-S. Joo, J.-H. Lee, E.-W. Lee, K.-D. Song, D.-D. Lee, in: *Proceedings of the 1st International Conference on Sensing Technology*, Palmerston North 2005, p. 307.